Laser Induced Breakdown Spectroscopy (LIBS) applied to stratigrafic elemental analysis and Optical Coherence Tomography (OCT) to damage determination of cultural heritage Brazilian coins

Marcello M. Amaral[a], Marcus P. Raele[a], Anderson Z. de Freitas[a], Guilherme S. Zahn[a], Ricardo E. Samad[a], Nilson D. Vieira Jr. [a], Luiz V. G. Tarelho[b]
[a]Nuclear and Energy Research Institute, IPEN / CNEN – SP, Av. Prof. Lineu Prestes, 2242, São Paulo, SP, BR 05508-900
[b]National Institute of Metrology, Standardization and Industrial Quality – INMETRO, Av. N. Sra. Das Graças, 50 –Duque de Caxias – RJ , BR – ZIP: 25250-020

ABSTRACT

This work presents a compositional characterization of 1939's Thousand "Réis" and 1945's One "Cruzeiro" Brazilian coins, forged on aluminum bronze alloy.

The coins were irradiated by a Q-switched Nd:YAG laser with 4 ns pulse width and energy of 25 mJ emitting at 1064 nm reaching $3.10^{10}Wcm^{-2}$ (assured stoichiometric ablation condition), forming a plasma in a small fraction of the coin. The plasma emission was collected by an optical fiber system connected to an Echelle spectrometer. The capability of LIBS to remove small fraction of material was exploited and the coins were analyzed ablating layer by layer from patina to the bulk.

The experimental conditions to assure reproductivity were determined by evaluation of three plasma paramethers: ionization temperature using Saha-Boltzmann plot, excitation temperature using Boltzmann plot, plasma density using Saha-Boltzmann plot and Stark broadening.

The Calibration-Free LIBS technique was applied to both coins and the analytical determination of elemental composition was employed. In order confirm the Edict Law elemental composition the results were corroborated by Neutron Activation Analysis (NAA). In both cases the results determined by CF-LIBS agreed to with the Edict Law and NAA determination. Besides the major components for the bronze alloy some other impurities were observed.

Finally, in order to determine the coin damage made by the laser, the OCT (Optical Coherence Tomography) technique was used. After tree pulses of laser 54μg of coin material were removed reaching 120μm in depth.

Keywords: LIBS, Laser Induced Breakdown Spectroscopy, OCT, Optical Coherence Tomography, NAA, Neutron Activation Analysis, Brazilian Coin.

1. INTRODUCTION

LIBS is a acronym for "Laser Induced Breakdown Spectroscopy" and is a technique that, as the name suggest, use a laser to generate plasma on a sample surface. Looking at the plasma emission (spectroscopy), one can determine which elements are present in this sample. Researches have developing LIBS to transform it into an analytical technique, the most common techniques (widely used in analytical chemistry) uses calibration standards and calibration curves to evaluate concentrations from the instrument signals. There is an alternative technique to analytically determine the sample composition and it is known as Calibration Free LIBS (CF-LIBS). This work presents the development of CF-LIBS for the analytical study of cultural heritage metallic material.The concentration results were confirmed by Neutron Activation Analysis (NAA) and laser damage depth were were evaluated by Optical Coherence Tomography (OCT). All this techniques applied to the samples are presented below.

1.1 LIBS

Since the beginning of laser development in the 60's, scientists explore all its potential application and as soon as first laser ablation was produced [1] the determination of sample composition using spectroscopy technique [2] was

discussed. But due to technological difficulties at that time this technique was left aside, returning in the 80's when laser and detection technologies [3] advanced enough. In 2005 [4] this technique using laser to ablate material sample and spectroscopy to determine atomic composition of a sample (solid, liquid or gaseous) has it name standardized as LIBS (Laser Induced Breakdown Spectroscopy).

As an analytical technique, LIBS presents some advantages to other techniques: no sample preparation, real time resuts, *in situ* analysis, low coast compared to other analytical techniques, chemical and biological sample identification in solid, liquid and gaseous form, and in many cases is a non destructive technique. The main disadvantage is the high limit of detection, about 500ppm but 1ppm can be reached for some elements [5].

LIBS is a very versatile technique and have been used in siderurgy [6], industrial process control [7], environmental geochemistry [8], biohazard material detection [9], forensic science [10], microbiology [11], odontology [12], archaeology [13], cultural heritage [14] and art conservation [15].

Specifically, LIBS has been used to determine elemental composition of cultural heritage bronze artifact [16, 17]. The main advantage of using LIBS in these studies is that it pulse of laser remove a small layer, allowing a stratigraphic analysis [14, 17].

LIBS Fundamentals

The LIBS technique uses a pulsed laser to remove and excite the sample material, generating a plasma with sample elements. The plasma can be understood as a third state of matter, were its constituents were dissociated, just in atomic and ionic form. When excited state electrons from atoms and ions change from more energetic states to a less energetic one, they emit photons and the energy of these photons are characteristics from the atoms or ions that they came from and measuring the plasma electronic emission spectrum allows one to determine the atoms and ions that compose the plasma [5].

The analytical LIBS technique is based on three assumptions. First the ablation is stoichiometric, the plasma has the same composition of the sample when irradiance (radiant exitance) exceeds 10^9 W/cm^2 [18]. Secondly, the spectral line emission are optically thin (absorption or self-absorption do not occur), this is achieved by right choice of observed lines. Finally, the third assumption is that the plasma is in Local Thermodynamic Equilibrium (LTE), at this condition in a small volume and in one instant the plasma follows the thermodynamic equations [19].

Plasma conditions and CF-LIBS

To guarantee the reproductivty of LIBS technique as an analytical technique, the excitation electronic temperature T, plasma electron density and ionization temperature has to be known.

Under LTE conditions, the excited states for each species present in the plasma follows the Boltzmann Distribution [5, 13, 20, 21]. Due to detectors features, the integrated intensity of spontaneous emission (I_{ij}) is proportional to Boltzmann distribution and transition probability (A_{ij}) from excited state *i* to *j* (equation 1) [16].

$$I_{ij} = \frac{F\, g_i\, A_{ij}}{U^s(T)} n^s e^{-E_i/kT} \tag{1}$$

were g_i is the statistical weight or state degenerescence of *i* upper energy state transition, E_i is the energy of *i* upper energy state transition, n^s is the total density (concentration) of *s* species (species refers to atomic or ionic state of a element), k is the Boltzmann constant and $U^s(T)$ is the partition function *s* species in electronic excitation temperature T.

Manipulating equation 1 and linearizated by using natural logarithm (equation 2) allows the construction of what is knows as Boltzmann Plot, where each observed transition in the spectrum corresponds to a point in the Plot.

$$\ln\left(\frac{I_{ij}}{A_{ij}\, g_i}\right) = \ln\left(\frac{F}{U^s(T)} n^s\right) - \frac{1}{kT} E_i \tag{2}$$

F is a normalization constant dependent on the experimental setup only.

Through this method a linear fit can be made and the electronic excitation temperature T of plasma can be determined through the angular coefficient. From linear coefficient of equation 2 the concentration n^s of each species can be determined. Atomic and ionic species of an element can have different electronic excitation temperature. However, to do a fitting, it is required observe at least two lines, but it doesn't occur in all cases. In order to determine the concentration of each observed element n^s, it was assumed that all the atomic species had the same electronic excitation temperature and all the ionic species had another electronic excitation temperature similar for all of them. This procedure is known as CF-LIBS (Calibration Free LIBS) and this method dismissed the use of calibration curves but is very sensitive to variations in the observed transition lines choice and presence of atomic and ionic species of elements.

The plasma electronic density can be determined using Stark Broadening (equation 3) when the observed line width (FWHM, $\Delta\lambda_{Stark}$) is known.

$$n_e = \frac{\Delta\lambda_{Stark}}{2\omega} 10^{16} \tag{3}$$

The third way to characterize the plasma is through Ionization Temperature using Saha-Boltzmann Plot [5, 16, 20, 21] that can be determined by a linearization of Saha-Boltzmann [16] equation 4, for using this method both atomic and ionic lines of the same element must be observed. The Ionization Temperature does not have the usual concept of temperature but is a measure of ionization fraction, it corresponds to which fraction of an element is in ionic and atomic state. Consequently, because different elements have different ionization potential, they will have different ionization fraction and then Ionization Temperature.

$$\ln\left(\frac{I_{ij}^{II} A_{mn}^{I}\, g_n^I}{I_{mn}^{I} A_{ij}^{II}\, g_i^{II}}\right) = \ln\left(\frac{2(2\pi m_e kT)^{3/2}}{n_e h^3}\right) - \left(\frac{E_{ion} + E_i^{II} - E_m^I}{kT}\right) \tag{4}$$

were the indices I and II refer to atomic and ionic states respectively.

1.2 OCT Technique

OCT is a technique based on low coherence length interferometry that lead to the development of Optical Coherence-Domain Reflectometry [22] method which was firstly applied to detect and locate optical fiber's faults [23]. The breakthrough of this technology was the application of low coherence interferometry to make tomographic images of delicate live structures, such as eyes structures [24, 25] and other biological tissue [26, 27].

Despite of OCT being an established diagnostic tool, especially in the biomedical area, it has less than two decades of conception, it is still on technological childhood. While research institutes are heavily investing time and resources on it to learn and improve the technique, at the same time, companies are commercializing them, with a small technological time lap between them. In others words this is a hint about the market acceptance and necessity for OCT systems even though the technology seems to be far from its saturation.

The most common OCT setup applied on commercial types is the Michelson interferometer using optical fibers. In this interferometer, the light is conducted by the optical fiber to a 2x2 couple and divided into two beams, part of the radiation, goes to a reference mirror and the other part goes to sample (Figure 1).

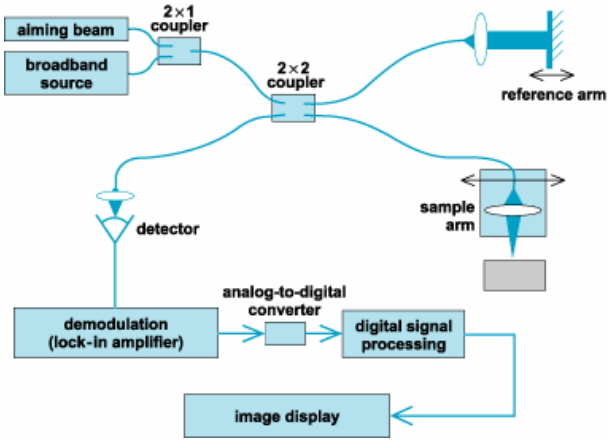

Fig. 1: Schematic OCT system used to coin damage measure.

The mirror and sample backscattering radiations recombine forming an interferometric pattern in the detector. Because the light source has low coherence length, broad spectral band, the interference occurs in the detector only when the optical length difference between sample's arm and reference arm is shorter than the coherence length, i.e., only the photons once scattered have the information necessary to generate the interferometrics pattern.

The lateral resolution of the system depends on the light source coherence length (*lc*).

$$lc = \frac{\lambda^2}{\Delta\lambda} \tag{3}$$

And for a Gaussian profile it can be written as:

$$\Delta z = \frac{2\ln 2}{\pi} lc \tag{4}$$

where Δz is the system longitudinal resolution, λ is the central wavelength of light source, and $\Delta\lambda$ is FWHM of source spectral band; the lateral resolution is determined by the beam waist after pass through a convergent lens.

1.3 NAA

Neutron Activation Analysis (NAA) is a multi elementary technique used even for qualitative analysis or quantitative analysis from major concentrations to trace elements. It is diffent from other analytic spectroscopic techniques because it is based on nuclear transitions instead electronics transitions.

In a NAA analysis the sample is irradiated with neutrons in the reactor core, the thermal neutron interacts with the sample elemental nucleus by inelastic collisions, causing the neutron capture. Sample elements radioisotopes are created, theses radioisotopes decay emitting particles followed by gamma emission, characteristic of emitter isotope. This emission is proportional to element concentration and makes it possible to determine the sample composition.

2. PROCEDURE

To perform this work two Brazilian coins were used (Figure 1), 1939 Thousand "Reis" and 1945 One "Cruzeiro". The coins had their composition determined by an Edict law width a description for their forge process. These coins were chosen because they have historical value but are easy to be found. The first step was to perform NAA technique analysis to confirm the coins composition determined by Edict -law (Table 1), then we passed to LIBS analysis.

(a) (b)

Fig. 2: Brasilian coins 1945 One "Cruzeiro" and 1939 Thousand "Reis", (a) averse (b) reverse of coins.

Table 1: Elemental Coins Composition defined by Edict –law.

Coin	Cu (%)	Al (%)	Zn (%)
1939's Thousand "Réis	90.0 (20)	8.0 (10)	2.5 (10)
1945's One "Cruzeiro"	90.0 (20)	8.0 (10)	2.0 (20)

In LIBS analysis we used a Nd:YAG Q-switched laser (Quantel Brilliant) operating at 1064nm wavelength, 4ns pulse width, the pulse energy was varied (25, 50, 75 and 100mJ). The laser beam was focused on the sample surface using a convergent lens with 20cm focal length, positioned at 20cm from the surface of the coin, the laser reach the sample forming a plasma. With this system the Irradiance reached from 3 10^{10}Wcm^{-2} to 1.25 10^{11} Wcm^{-2}. The plasma emissions were collected by an optical fiber and conducted to an Echelle spectrometer "ESA 3000"' (LLA Instruments) with resolution of 0,02nm, from 200 to 600nm. The time delay between laser pulse and acquisition of plasma emission signal (600ns, 1, 2, 5 e 10µs), and the integration time of spectrum (500 ns, 2 e 5µs) was varied to determine the better experimental conditions. The interface between laser, spectrometer and data acquisition was made by a software that also provided an initial identification of line transitions observed. Figure 8 show schematical experimental setup. This study was performed laser pulse per laser pulse, it turns out possible to apply a stratigrafic elemental analysis because laser remove a small part of material. Moreover, it was studied some region of the 1939 Thousand "Réis" Brazilian coin that presents visual difference, these regions were classified as Patina, Consumed (to looks like a hands manipulated), Anverse and Revese of coin.

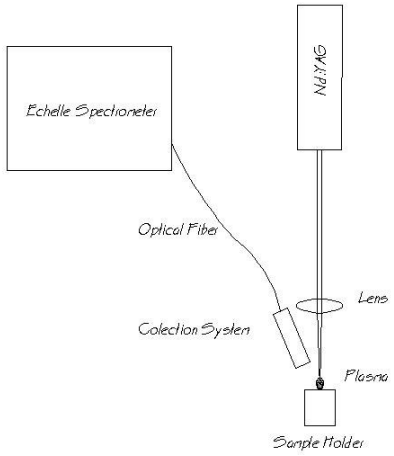

Fig. 2: Schematical experimental setup used in LIBS technique.

To determine the laser damage on surface coin, it was used a commercial type OCT (OCP930SR ThorLabs) with axial

and lateral resolution of 6μm to take a series of cross sections images were perform of the surface, and using image manipulation software reconstruct the surface, permitting to calculate the volume and the depth of the damage.

3. RESULTS

3.1 NAA Results

In order to confirm the Edict-law that determines the aluminum bronze alloy of coins forge, a NAA was performed in 1945's cruzeiro coin. The sample was irradiated in the IEA-R1 reactor of Nuclear and Energy Research Institute (IPEN-CNEN/SP - Brazil). Due to radioisotopes features just the mass ratio of major elements (Al/Cu) could be determined, the value founded for this ratio was 0.0811(9), i.e., in the material we have 92.50(8) % of Copper and 7.50(8) % of Aluminum. The founded results confirm the forge material composition.

3.2 LIBS Experimental conditions

Using the system described in the previous section, the plasma emission was measured under the several possible conditions of energy pulse, time delay and integration time. A study of the signal-to-noise ratio from all the experimental conditions combination was made, and the optimized conditions were: pulse energy of 25mJ (3 10^{10}Wcm^{-2}), 2μs of time delay and 1μs of integration time. Under these conditions the spectra were analyzed to identify the elements present in the sample through the line observed.

3.3 OCT

When a measurement is made on a cultural heritage material, evaluate the damage (caused by the technique) evaluation is very important to decide which technique will be used. The OCT technique was perform to evaluate the damage caused by the laser and determines the thickness of each layer (equivalent to one laser pulse). The coin from 1939 (Thousand "Réis") was used in this study of damage evaluation after it be reached by three 25mJ laser pulses. A series of images were taken and using a image treatment software a 3D image was constructed (Figure 3).

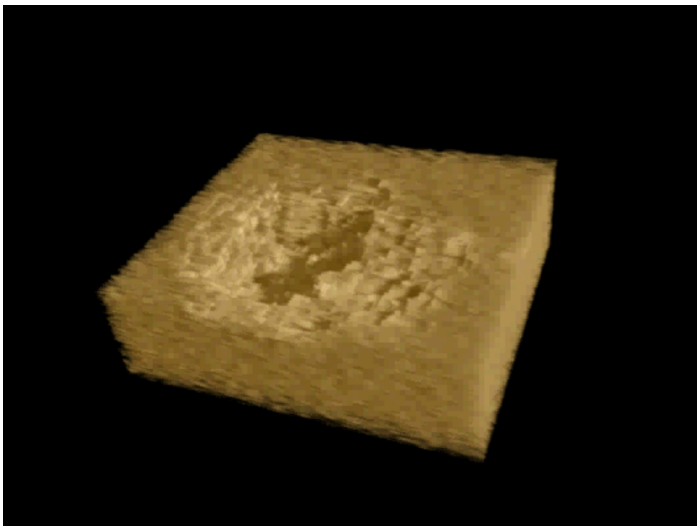

Fig.3: 3D reconstructed image of Laser damage on 1939's Thousand "Réis" coin surface.

The damage volume was determined, 8 10^{-3}mm^3, it is equivalent to 54μg of material, reaching 120μm depth after three laser pulses, then each laser pulse is equivalent to a 40μm depth layer.

3.4 LIBS measurements

Figure 4 presents an example of the measured spectra and the identification of lines in the data acquisition software.

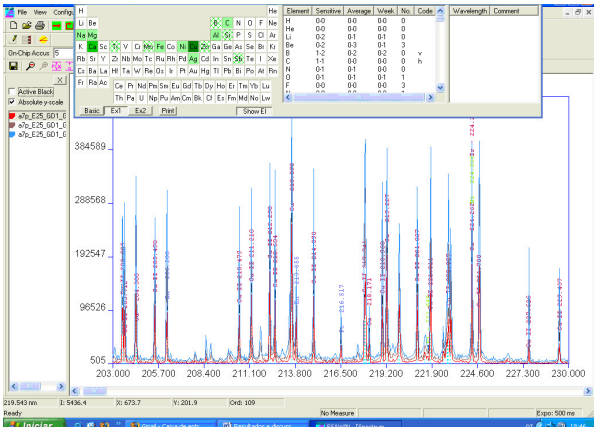

Fig. 4: Example of measured spectra and the identification of lines in the data acquisition software

The elements spectroscopically identified are presented in Table 2, in this table can be observed the presence of both forge material and possible impurities or incrustation due coin manipulation can be observed in this table.

Table 2: Elements identify by spectral emission, both nominal forge material and possible impurity or incrustation.

Forge Material	Possible Impurity or Incrustation	
Cu	Ca	Ti
Al	Na	Mn
Zn	Mg	B
	Fe	Si
		Ni

After the identification of the observed lines provided by software using a home made worksheet permitted the determination of plasma conditions. The first condition measured was the plasma electronic density, for this purpose it was used 394.4 and 396.1nm Al lines and equation 3. Lorentzian fit was done on the Al observed line to determine the FWMH of the transition. The average electronic plasma density was 1.94 (4) 10^{16}cm^{-3} and 2.29 (35) 10^{16}cm^{-3} for 1945's One "Cruzeiro" and 1939's Thousand "Réis" coins respectively.

The plasma electronic excitation temperature was determined by a Boltzmann Plot using the observed transitions line from Cu (both atomic and ionic), because it was the element that provided much more observed lines making possible a better linear fit. Figure 5 shows an example of Boltzmann Plot (Thousand "Reis" Brazilian coin anverse region).

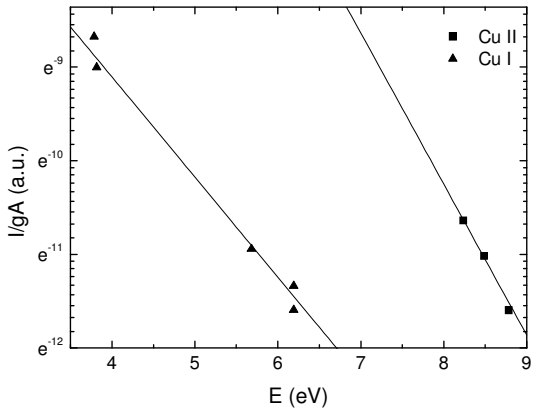

Fig. 5: Boltzmann Plot example of Thousand "Reis" Brazilian coin anverse region, Cu I is the atomic species and Cu II is the ionic species

The average electronic excitation temperature for 1945's One "Cruzeiro" coin was 9900(1400)K and 7100(300)K for atomic and ionic respectively, and for 1939's thousand "Réis" coin it was 10800(1600)K and 6800(1600)K for atomic and ionic respectively.

The Temperatures determined by Boltzmann Plot are related to the slope of the linear fit, assuming that atomic elements species had the same temperature that the copper atomic species (Cu I), or the fit had the same slope. A linear fitting was made for all the other atomic elements species. Therefore parallel lines to the Cu I fit were fitted to determine the linear coefficient, which with equation 2 for CF-LIBS, could be used to determine the elements concentration. The same process was made to the ionic species using the slope of copper ionic species (Cu II). Figure 6 presents an example of these parallel lines used to determine the linear coefficient and consequently elements concentration:

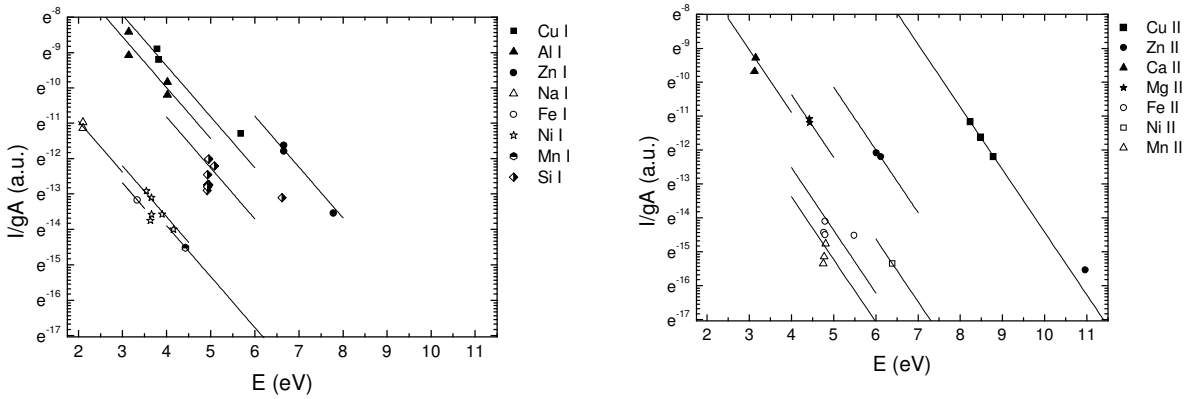

Fig. 6: Boltmann Plot of Consumed region in 1939's 1000 "Réis" used to determine the coin elemental concentration.

Observing the elemental concentration values found to 1945's One "Cruzeiro" coin in the 400µm depth layer (97.2(19)% of Cu, 0,046 (22)% of Al and 2,7 (5) % of Zn), where just forge elements were observed, and comparing it with forge material nominal value and NAA measurement, it can be noted that some discrepant value of Al concentration occurs.

The CF-LIBS is extremely sensitive to observation of atomic and ionic transition line, i.e., if no ionic lines are observed

(like in Al case) the proportion of element can be drastically changed.

Looking at average ionization temperature, 1100 (3500) K for Cu and 8500(990) K for Zn, it corresponds to 99.5(5)% in the ionized fraction of each element, in contrasting with the ionization process expected for the electronic excitation temperature achieved. This indicates that occurred non-thermal process in the plasma like energy changes by collision.

This behavior could explain the low Al concentration, because Al has 5.98eV ionization potential, while Cu and Zn have 7.73 and 9,39eV, and as Cu and Zn, Al could be in the same ionization fraction. The problem of observing none Al ionic line is due to experimental limitation (incapability to measure below 200 nm in spectral range). Assuming that Al had the same average ionization fraction as Cu e Zn, a correction to the concentration needs to be made.

The coins elemental concentration are presented in Table 3 and 4 for 1945's One "Cruzeiro" and 1939's Thousand "Réis" respectively, in each studied region and stratigrafic layer.

Table 3: Elemental Concentration of coins constituents of 1945's One "Cruzeiro" on analyzed layers, after non-thermal ionization fraction correction.

Element	Concentration (%)					
	40µm	80 µm	120 µm	160 µm	200 µm	400 µm
Cu	89.0 (11)	86,5 (5)	86,5 (6)	90,9 (8)	88,8 (8)	89,0 (17)
Al	8.08 (12)	9,85 (7)	10,88 (9)	7,09 (18)	9,1 (10)	8 (4)
Zn	1.09 (17)	2.00 (12)	1.74 (12)	1.82 (16)	1.9 (6)	2.5 (5)
Ca	0.129 (3)	0.0852 (19)	0.030 (4)	0.0107 (22)	0.0082 (15)	-
Na	0.651 (5)	0.1307 (16)	0.1614 (28)	-	-	-
Mg	0.309 (6)	0.1922 (19)	0.0730 (10)	0.0277 (8)	0.0172 (7)	-
Fe	0.71 (7)	0.59 (6)	0.22 (10)	-	-	-
Ti	-	0.23 (5)	0.16 (3)	0.13 (5)	0.14 (8)	-
Mn	0.0098 (16)	-	0.0200 (19)	-	-	-
Si	0.0138 (13)	0.46 (9)	0.19 (4)	-	-	-

As can be seen in Table XX1 when the laser penetrates in the coin removing layer by layer, the presence of incrustation decreases until just forge material is observed. This behavior is less perceptible in Table XX because the penetration is not so deep.

4. CONCLUSIONS

The study of 1939's Thousand "Réis" and 1945's One "Cruzeiro" Brazilian coins forged on aluminum bronze alloy using a Q-switched Nd:YAG laser with 4 ns pulse width emitting at 1064 nm, allowed determination of experimental conditions to apply LIBS Technique and CF-LIBS method on the cultural heritage metallic material

The established value of pulse energy was 25mJ that associated to a 20cm focal length lens reached 3.10^{10}Wcm^{-2} (assure stoichiometric ablation condition). The plasma generated by laser was spectroscopically analyzed using an Echelle spectrometer. The capacity of LIBS to remove small portions of sample material allowed a stratigrafic analysis. To determine the laser damage on coin surface and the depth of each layer in the stratigrafic analysis, OCT technique imaged the damage. After three laser pulses 54µg of material was removed reaching 120µm depth.

To guarantee the reproductivity of the technique the plasma was characterized by Electronic Excitation Temperature using Boltzmann Plot, plasma electronic density using Stark broadening and Ionization Temperature using Saha-Boltzmann Plot.

The NAA was used to corroborate the results and confirm the Edict-Law elemental composition. CF-LIBS associated to a correction by ionization fraction was used to determine coins elemental composition. In both coins the results determinated by CF-LIBS agree with the Edict Law and NAA determination. Besides the major components for the bronze alloy some other impurities were observed

Table 4: Elemental Concentration of coins constituents of 1939's Thousand "Réis" on analyzed layers, after non-thermal ionization fraction correction.

Element	Concentration (%)					
	Patina			Consumed		
	40µm	80 µm	120 µm	40µm	80 µm	120 µm
Cu	88.5 (19)	90.0 (9)	91.5 (6)	85.4 (14)	89.5 (5)	90.2 (6)
Al	7.83 (8)	6.65 (5)	7.07 (4)	12.0 (3)	8.31 (5)	7.02 (22)
Zn	1.28 (16)	2.29 (13)	0.90 (4)	1.24 (16)	1.75 (5)	2.44 (11)
Ca	0.105 (7)	0.050 (5)	0.0165 (14)	0.099 (5)	0.0129 (10)	0.007 (4)
Na	1.252 (6)	0.3824 (23)	0.2599 (17)	0.1523 (15)	0.0318 (3)	0.0166 (4)
Mg	0.236 (8)	0.1475 (24)	0.0471 (5)	0.137 (4)	0.0370 (4)	0.0209 (5)
Fe	0.24 (6)	0.37 (6)	0.17 (4)	0.40 (8)	0.25 (2)	0.26 (5)
Ni	0.45 (8)	-	-	0.52 (5)	-	-
Ti	0.070 (18)	-	-	-	-	-
Mn	0.0100 (22)	0.044 (6)	0.0272 (24)	0.033 (4)	0.062 (4)	0.066 (8)
B	0.00330 (23)	-	-	-	-	-
Si	0.0158 (29)	0.023 (4)	-	0.088 (12)	-	-
	Reverse			Anverse		
	40µm	80 µm	120 µm	40µm	80 µm	120 µm
Cu	86 (4)	82.3 (9)	85.2 (7)	89.7 (22)	84.3 (6)	90.4 (6)
Al	10.13 (7)	12.8 (6)	9.81 (4)	8.24 (8)	11.22 (17)	7.89 (4)
Zn	1.45 (39)	3.31 (22)	3.68 (21)	1.14 (21)	2.98 (13)	1.29 (5)
Ca	0.147 (14)	0.117 (9)	0.084 (4)	0.054 (4)	0.1489 (24)	0.0221 (8)
Na	0.555 (4)	0.235 (12)	0.306(3)	0.512 (3)	0.2671 (17)	0.1435 (15)
Mg	0.361 (27)	0.221 (4)	0.1973 (28)	0.133 (5)	0.247 (3)	0.0377 (5)
Fe	0.9 (3)	0.74 (11)	0.54 (8)	0.23 (5)	0.61 (6)	0.17 (4)
Ni	0.0019 (3)	-	-	-	-	-
Ti	0.118 (28)	-	-	-	-	0.010 (4)
Mn	0.076 (13)	0.181 (11)	0.156 (12)	0.0206 (29)	0.137 (8)	0.050 (7)
B	-	0.0103 (6)	-	-	0.00589 (23)	-
Si	0.0129 (7)	0.027 (4)	0.0265 (24)	0.00206 (23)	0.0396 (29)	0.0050 (13)

REFERENCES

[1] BRECH, F; CROSS, L. Appl. Spectrosc., v. 16, p. 59, 1962.

[2] RUNGR, E.F.; MINCK, R.W.; BRYAN, FR. Spectr. Chim. Acta B, v. 20, p. 733, 1964.

[3] SANTOS Jr., D.; TARELHO, L.V.G.; KRUG, F.J.; MILORI, D.M.B.P.; MARTIN NETO, L.; VIEIRA Jr., N.D. Espectroscopia de Emissão Óptica com Plasma Induzido por Laser (LIBS) - Fundamentos, Aplicações e Perspectivas. Revista Analytica, n. 24, p. 72, 2006.

[4] Noll, R; Terms and Notations for Laser-Induced Breakdown Spectroscopy; Anal. Bioanal. Chem., v.385, p. 214, 2006.

[5] CREMERS, D.A.; RADZIEMSKI, L.J. Handbook of Laser-Induced Breakdown Spectroscopy. John Wiley \& Sons; England; 2006.

[6] STURM, V.; VRENERGOR, J.; NOLL, R.; HEMMERLIN, M. Bulk analysis of steel samples with surface scale layers by enhanced laser ablation and LIBS analysis of C, P, S, Al, Cr, Cu, Mn and Mo. \textit{J. Anal. At. Spectrom.}, v. 19, p. 451, 2004.

[7] BULAJIC, D.; \textit{et al}. Diagnostico f high-temperature steel pipes in industrial environment by laser-induced breakdown spectroscopy technique: the LIBSGRAIN project; Spectr. Chim. Acta B, v. 57, p. 1181, 2002.

[8] CANEVE, L.; CALÃO, F.; FABBRI, F.; FANTONI, R.; SPIZZICHINO, V.; STRIBER, J. Laser-induced Breakdown spectroscopy analysis of asbestos. Spectr. Chim. Acta B, v. 60, p. 1115, 2005.

[9] MUNSON, C.A.; DE LUCIA Jr., F.C.; PIEHLER, T.; McNESBY, K.L.; MIZIOLEK, W.; Investigatio of statistics stratedies for improving the discriminating power of laser-induced breakdown spectroscopy for chemical and biological warfare agent simulants. Spectr. Chim. Acta B, v. 60, p. 1217, 2005.

[10] DOCKERY, C.R.; GOODE, S.R. Laser-induced breakdown spectroscopy for detection of gunshot residues on the hands of a shooter; Applied Optics, v. 42, p. 6153, 2003.

[11] BEDDOWNS, D.C.S.; TELLE, H.H. Prospects of real-time single-particle biological aerosol analysis: A comparison between laser-induced breakdown spectroscopy and aerosol time-of-flight mass spectrometry. Spectr. Chim. Acta B, v. 60, p. 1040, 2005.

[12] SAMEK, O.; TELLE, H.H.; BEDDOWNS, D.C.S. Laser-induced breakdown spectroscopy: tool for real-tiem, in vitro and in vivo identification of carious teeth; BMC Oral Health; v. 1, p. 1, 2001.

[13] FORNARINI, L.; SPIZZICHINO, V.; COLAO, F.; FANTONI, R.; LAZIC, R. Influence of laser wavelength on LIBS diagnostics applied to the analysis of ancient bronzes; Anal. Bioanal. Chem., v.385, p. 281, 2006.

[14] POULI, P.; MELESSANAKI, K.; GIAKOUMAKI, A.; ARGYROPOULOS, V.; ANGLOS, D.; Measuring the thickness of protective coatings on historic metal objects using nanosecond and femtosecond Laser induced breakdown spectroscopy depth profiling; Spectr. Chim. Acta B, v. 60, p. 1163, 2005.

[15] OUJJA, M.; VILA, A.; REBOLLAR, E.; GARCÍA, J.F.; CASTELLEJO, M. Identification of inks and structural characterization of contemporary artistic prints by laser-induced breakdown spectroscopy. Spectr. Chim. Acta B, v. 60, p. 1140, 2005.

[16] MIZIOLEK, A; PALLESCHI, V; SCHECHTER, I; Laser-Induced Breakdown Spectroscopy (LIBS): Fundamentals and Applications. Cambridge: Cambridge, 2006.

[17] COLAO, F.; \textit{et al}. Laser-induced breakdown spectroscopy for semi-quantitative and quantitative analyses of artworks - application on multi-layered ceramics and copper based alloys; Spectr. Chim. Acta B; v. 57, p. 1219, 2002.

[18] CHAN, W.T.; RUSSO, R.E. Study of laser-material interactions using inductively coupled plasma-atomic emission spectrometry. Spectr. Chim. Acta B, v. 46, p. 1471, 1991.

[19] RADIVOJEVIC, I. Spectrochemical Analysis of Solid Samples by Laser-induced Plasma Spectroscopy. 2004. Tese (Doutorado), Technischen Universität München, Munique.

[20] TOURIN, R.H.; Spectroscopic Gas Temperature Measurement. Amsterdam: Elsevier, 1966.
[21] Lochte-Holtgreven, W; Plasma Diagnostics. New York, N.Y.: AIP Press, 1995
[22] Youngquist, R.C., Carr, S. and Davis, D.E.N. ,"Optical coherence-domain reflectometry: A new optical evaluation technique", Opt. Lett. 12, 158-160 (1987).
[23] Takada, K., Yokohama, I., Chida, K. and Noda, J. , "New measurement system for fault location in optical waveguide devices based on an interferometric technique", Appl. Opt. 26, 1603-1606 (1987).
[24] Huang, D., Swanson, E.A., Lin, C.P., et al. , "Optical coherence tomography", Science, 254, 1178–1181 (1991).
[25] Fercher, A. F., Mengedoht, K. and Werner, W. , "Eye-length measurement by interferometry with partial coherent light", Opt. Lett. 13, 1867-1869 (1988).
[26] Clivaz, W., Marquis-Weible, F., Salathe, R. P., Novak, R. P. and Gilgen, H. H. , "High-resolution reflectometry in biological tissue", Opt. Lett. 17, 4-6 (1992).
[27] Schimitt, J. M., Knüttel, A. and Bonner, R. F. , "Measurement of optical properties of biological tissues by low-coherence reflectometry", Appl. Opt. 32, 6032-6042 (1993).